J|A|C|S
ARTICLES
Published on Web 03/09/2006

CP/MAS ^{13}C NMR Characterization of the Isomeric States and Intermolecular Packing in Tris(8-hydroxyquinoline) Aluminum(III) (Alq_3)

Hironori Kaji,*[,†,‡] Yasunari Kusaka,[†] Goro Onoyama,[†,§] and Fumitaka Horii[†]

Contribution from the Institute for Chemical Research, Kyoto University, Uji, Kyoto 611-0011, Japan, and PRESTO, Japan Science and Technology Agency (JST), 4-1-8 Honcho Kawaguchi, Saitama 332-0012, Japan

Received September 25, 2005; E-mail: kaji@scl.kyoto-u.ac.jp

Abstract: The isomeric states and intermolecular packing of tris(8-hydroxyquinoline) aluminum(III) (Alq_3) in the α-, γ-, and δ-crystalline forms and in the amorphous state, which are important for understanding the light-emitting and electron-transport properties, have been analyzed by CP/MAS ^{13}C NMR. This simple NMR experiment shows that the isomeric state of α- and amorphous Alq_3 is meridional, whereas that of γ- and δ-Alq_3 is facial. In the amorphous Alq_3, the inclusion of facial isomers has been under debate. Our experiments show that meridional isomers are dominant in the amorphous Alq_3, although the existence of facial isomers cannot be completely denied. The local structure of amorphous Alq_3 is similar to that of α-Alq_3 and is significantly different from those of γ- and δ-Alq_3. Among these Alq_3 samples, the effect of intermolecular interaction is not found only for γ-Alq_3. This finding can explain the good solvent solubility of γ-Alq_3, compared with the other crystalline forms. It is also shown that the structures are locally disordered not only for amorphous Alq_3 but also for α-Alq_3, although clear X-ray diffraction peaks are observed for α-Alq_3. In contrast, the local structures of γ- and δ-Alq_3 are well defined. A clear relation is found between the spectral patterns of CP/MAS ^{13}C NMR and the fluorescence wavelengths; the samples, which consist of facial isomers, show blue-shifted fluorescence compared with those of meridionals.

Introduction

Since 1987,[1] tris(8-hydroxyquinoline) aluminum(III) (Alq_3) has been the most extensively used light-emitting electron-transport material in organic light-emitting diodes (OLEDs). In Alq_3, two different isomeric forms exist, meridional and facial isomers, as shown in Figure 1. The existence of these isomers is of particular interest in terms of the electron-transport properties, because the energy difference for electron injections in meridional and facial Alq_3 molecules is estimated to be 0.07 eV by the density functional theory (DFT) calculations, and the minor facial components are assumed to act as efficient traps in the electron transport process.[2]

Quantitative estimation of the meridional/facial ratio in the sublimed amorphous Alq_3 films was carried out by Malliaras et al.[3] based on electron mobility measurements, and they concluded the existence of facial isomers to be a minor contribution. However, this estimation was carried out based on the effective dipole moment, and the meridional and facial isomers were not directly observed. In contrast, Kushto et al.[4] observed no spectral evidence for the presence of facial isomers from matrix-isolation infrared spectroscopy. On the basis of the measurements of the Alq_3 sublimed films with different purities, Malliaras et al.[3] experimentally showed that well-purified Alq_3 shows nondispersive transport, indicating that the traps in the Alq_3 films are not intrinsic. These two experiments suggest that the facial isomers are not included in the amorphous films. A clear spectroscopic observation of meridional and facial isomers

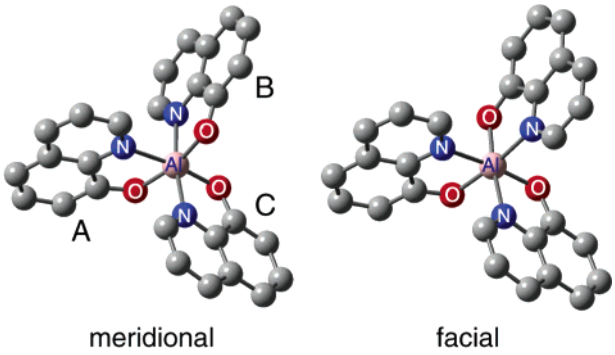

Figure 1. Two isomeric forms of Alq_3 molecules, meridional and facial. Hydrogen atoms are omitted for clarity. In the facial isomer, the three ligands are equivalent, while they are different as labeled by A, B, and C in the meridional isomer.

† Kyoto University.
‡ PRESTO, JST.
§ Present address: Ministry of Education, Culture, Sports, Science and Technology (MEXT), 2-5-1 Marunouchi Chiyoda-ku, Tokyo 100-8959, Japan.

(1) Tang, C. W.; VanSlyke, S. A. *Appl. Phys. Lett.* **1987**, *51*, 913−915.
(2) Curioni, A.; Boero, M.; Andreoni, W. *Chem. Phys. Lett.* **1998**, *294*, 263−271.
(3) Malliaras, G. G.; Shen, Y.; Dunlap, D. H.; Murata, H.; Kafafi, Z. H. *Appl. Phys. Lett.* **2001**, *79*, 2582−2584.
(4) Kushto, G. P.; Iizumi, Y.; Kido, J.; Kafafi, Z. H. *J. Phys. Chem. A* **2000**, *104*, 3670−3680.

10.1021/ja0565774 CCC: $33.50

will settle this controversy; however, the observation has been difficult, mainly because Alq_3 in OLEDs is in the amorphous state.

Even the crystal structures of pure Alq_3 have not been identified for a long time. The crystal structures of pure Alq_3 were first determined by Brinkmann et al.[5] in 2000. They found three polymorphs, α-, β-, and γ- Alq_3; the crystal structure of β-Alq_3 was determined by a single crystal X-ray diffraction, and it was clearly found that β-Alq_3 was composed of meridional isomers. The crystal structure of α-Alq_3 was determined by the Rietveld analysis of powder X-ray diffraction patterns, and this crystalline form was also shown to be formed by meridional isomers. Brinkmann et al. suggested that γ-Alq_3 was formed by orientationally disordered meridional isomers, although the crystal structure was not well identified. On one hand, Muccini et al.[6] and our group[7] suggested that γ-Alq_3 consisted only of facial isomers.

The isomeric states of Alq_3 are considered to be crucial also for the light-emitting properties. In 2001, another crystalline form, δ-Alq_3, was found by Braun et al.[8] All the following studies[7−14] showed that δ-Alq_3 was in the facial form. δ-Alq_3 emits blue luminescence and the quantum yield is very high.[11] These results suggest that the isomeric state is a key factor in the fluorescence wavelength and the quantum yield. The DFT calculation also predicts the blue-shift fluorescence, where the HOMO−LUMO gap of a facial Alq_3 molecule is 0.3 eV wider than that of the meridional Alq_3.[2] The intermolecular interaction is another possible origin of the difference in the light-emitting properties, because the intermolecular $\pi-\pi$ orbital overlaps of 8-hydroxyquinoline ligands in δ-Alq_3 are weaker compared to α- and β-Alq_3 as pointed out by Cölle et al.[10] Brinkmann et al. suggest the $\pi-\pi$ orbital overlaps[5] or sample densities[15] to be the origin of the change in fluorescence wavelengths.

Solid-state NMR is one of the candidates for obtaining spectroscopic evidence of the isomeric states in Alq_3. The solid-state ^{27}Al NMR experiments by Utz et al.[13] report that α- and δ-Alq_3 are composed of meridional and facial isomers, respectively. Our solid-state ^{27}Al NMR experiments[7] support the results of Utz et al.[13] Our data also show that the isomeric state of γ-Alq_3 is facial. In addition, the amorphous Alq_3 is suggested to be predominantly meridional.

In this study, solid-state cross polarization/magic angle spinning (CP/MAS) ^{13}C NMR measurements have been carried out for crystalline Alq_3 in different polymorphs and for amorphous Alq_3. One of our purposes is the identification of the isomeric mixing state in amorphous Alq_3, which is crucial for the understanding of the properties of Alq_3 in OLEDs. Because the isomeric states of α- and δ-Alq_3 are already found to be meridional and facial, respectively,[5,7−14] the spectral patterns distinctive of meridional and facial Alq_3 isomers would be obtained from the CP/MAS ^{13}C NMR measurements of the two Alq_3 samples. These measurements enable us to determine the isomeric state in amorphous Alq_3. Another purpose of this study is the isomeric identification of γ-Alq_3. We will show clear evidence that γ-Alq_3 is composed of facial isomers.

We have also investigated the intermolecular interaction and the local structural disorder in these Alq_3 samples. A recent study by Lin et al.[16] shows that the intermolecular packing in Alq_3 has a significant effect on the carrier transport integral, H_{ab}, in the Marcus theory,[17−20] and they conclude that the intermolecular packing is the most crucial factor in the carrier transport in Alq_3. Because the CP/MAS ^{13}C NMR spectra are affected not only by the intramolecular isomeric states but also by the intermolecular packing, the difference of intermolecular packing in the respective Alq_3 samples are discussed based on the experimental spectra. The findings on the intramolecular and intermolecular interactions will provide insight into the origin of different fluorescence wavelengths in respective Alq_3 samples. Local structural disorders are found for α- and amorphous Alq_3. In contrast, the disorder is not observed in γ-Alq_3, which is contradictory to the suggestion in ref 5. The disorder is also not observed in δ-Alq_3. Finally, a close relation between the isomeric state and the fluorescence wavelength will be shown.

Experimental Section

Sample Preparation and X-ray Diffraction Measurements. Three crystalline Alq_3 samples in the α, γ, and δ forms, and one amorphous Alq_3 sample were used in this study. The α-Alq_3 was prepared by train sublimation of freshly synthesized Alq_3. The γ-Alq_3 was obtained by thermal annealing of α-Alq_3 at 407 °C for 10 s. The δ-Alq_3 was obtained by thermal annealing of α-Alq_3 at 400 °C for 30 min. The δ-Alq_3 thus obtained was contaminated by γ-Alq_3. However, pure δ-Alq_3 was prepared by washing the crude δ-Alq_3 with an excess of $CHCl_3$ and drying under vacuum for 1 day, because γ-Alq_3 was more soluble in $CHCl_3$ than δ-Alq_3. The amorphous Alq_3 was prepared by quenching the α-Alq_3 from 425 °C. For the preparation of γ-, δ-, and amorphous Alq_3, a pressure of 30 MPa was applied to make the temperature uniform and to avoid vaporization of the samples. All the procedures of thermal annealing and train sublimation were carried out under nitrogen gas or nitrogen gas flow. The respective polymorphs were identified by wide-angle X-ray diffraction (WAXD) measurements on a Rigaku RINT2000 diffractometer using Cu-$K\alpha$ radiation under the condition of 300 mA and 40 kV. The step angle was 0.02° and the scan range was 3−35°. The sampling time was 1.0 s. The diffraction patterns of α- and δ-Alq_3 agreed with those of α-Alq_3 in refs 5 and 8 and those of δ-Alq_3 in refs 10 and 11, respectively. Although no experimental WAXD diffractograms were found for pure γ-Alq_3, the pattern of γ-Alq_3 in this study agreed with all the possible X-ray peaks calculated by Cölle et al.[11] using the unit cell parameters reported by Brinkmann et al.[5] For amorphous Alq_3, only an amorphous halo was observed, and no sharp diffractions were detected.

Fluorescence Measurements. Fluorescence measurements have been performed at room temperature on a HORIBA SPEX Fluorolog-

(5) Brinkmann, M.; Gadret, G.; Muccini, M.; Taliani, C.; Masciocchi, N.; Sironi, A. *J. Am. Chem. Soc.* **2000**, *122*, 5147−5157.
(6) Muccini, M.; Loi, M. A.; Kenevey, K.; Zamboni, R.; Masciocchi, N.; Sironi, A. *Adv. Mater.* **2004**, *16*, 861−864.
(7) Kaji, H.; Kusaka, Y.; Onoyama, G.; Horii, F. *Jpn. J. Appl. Phys.* **2005**, *44*, 3706−3711.
(8) Braun, M.; Gmeiner, J.; Tzolov, M.; Coelle, M.; Meyer, F. D.; Milius, W.; Hillebrecht, H.; Wendland, O.; Schutz, J. U. V.; Brütting, W. *J. Chem. Phys.* **2001**, *114*, 9625−9632.
(9) Amati, M.; Lelj, F. *Chem. Phys. Lett.* **2002**, *358*, 144−150.
(10) Cölle, M.; Dinnebier, R. E.; Brütting, W. *Chem. Commun.* **2002**, *23*, 2908−2909.
(11) Cölle, M.; Gmeiner, J.; Milius, W.; Hillebrecht, H.; Brütting, W. *Adv. Funct. Mater.* **2003**, *13*, 108−112.
(12) Amati, M.; Lelj, F. *J. Phys. Chem. A* **2003**, *107*, 2560−2569.
(13) Utz, M.; Nandagopal, M.; Mathai, M.; Papadimitrakopoulos, F. *Appl. Phys. Lett.* **2003**, *83*, 4023−4025.
(14) Cölle, M.; Brütting, W. *Phys. Stat. Sol. (A)* **2004**, *6*, 1095−1115.
(15) Brinkmann, M.; Fite, B.; Pratontep, S.; Chaumont, C. *Chem. Mater.* **2004**, *16*, 4627−4633.
(16) Lin, B. C.; Cheng, C. P.; You, Z.-Q.; Hsu, C.-P. *J. Am. Chem. Soc.* **2005**, *127*, 66−67.
(17) Marcus, R. A. *J. Chem. Phys.* **1956**, *24*, 966−978.
(18) Marcus, R. A. *Annu. Rev. Phys. Chem.* **1964**, *15*, 155−196.
(19) Marcus, R. A. *J. Chem. Phys.* **1965**, *43*, 679−701.
(20) Marcus, R. A.; Sutin, N. *Biochim. Biophys. Acta* **1985**, *811*, 265−322.

3−22. The excitation wavelength was 350 nm, and the scanning range was 370−650 nm at a step of 1 nm with a sampling time of 0.2 s.

Solution NMR Experiments. Solution ^{1}H and ^{13}C NMR measurements were conducted on a JEOL AL 400 spectrometer operating under a static magnetic field of 9.4 T. $CDCl_3$ was used as a solvent, and measurements were carried out at 23 °C unless otherwise noted. The assignments of the solution ^{13}C NMR resonance lines were carried out by a ^{13}C−^{1}H correlation spectroscopy (CH−COSY) experiment based on the results of the solution ^{1}H NMR spectrum. The distortionless enhancement by a polarization transfer (DEPT) 45° experiment confirms the distinction of CH carbons and quaternary carbons in Alq_3. The direct assignment by a ^{13}C incredible natural abundance double quantum transfer experiment (INADEQUATE) failed due to the low signal/noise ratio. The assignments of the solution ^{1}H NMR resonance lines were originally carried out by Baker and Sawyer.[21] However, their spectral pattern is significantly different from our solution ^{1}H NMR pattern, therefore, we cannot use their assignments. Our pattern is consistent with that recently reported by Utz et al.[22] where the resonance lines are partly assigned. Here, we carried out ^{1}H−^{1}H correlation spectroscopy (COSY) and nuclear Overhauser effect (NOE) experiments in order to assign all the resonance lines. The ligand assignments, that is, which resonances correspond to which of the ligands, A, B, and C in Figure 1, are carried out by DFT calculations shown below, which cannot be clarified experimentally. The assignments based on the DFT calculations agree well with those based on the experiments except for C5A and C5C. See the Supporting Information for details of the assignments.

Solid-State NMR Experiments. CP/MAS ^{13}C NMR measurements were conducted on a Chemagnetics CMX-400 Infinity spectrometer operating at a ^{13}C frequency of 100.28 MHz (under a static magnetic field of 9.4 T). A double resonance probe with a 7.5 mm MAS probehead was used. The powdered samples were packed into zirconia rotors under an inert atmosphere of nitrogen. The ^{1}H and ^{13}C field strengths $\gamma B_1/2\pi$ of 62.5 kHz were used for the CP process, and the contact time was 5.0 ms. The dwell time and the acquisition time were 16.67 μs and 34.14 ms, respectively. The ^{1}H−^{13}C dipolar coupling was relatively strong and a time proportional phase modulation (TPPM) ^{1}H dipolar decoupling with the ^{1}H field strength of 83.3 kHz was applied during the detection of free induction decay. The optimized pulse width and the phase shift for TPPM scheme were 6 μs and 15°, respectively. The ^{13}C chemical shifts were expressed as values relative to tetramethylsilane (Me_4Si) using the CH_3 resonance line at 17.36 ppm for hexamethyl benzene crystals as an external reference. The MAS spinning speed was set to 6 kHz (±2 Hz), and the experiments were carried out at 23 °C throughout this work.

DFT Calculations. Molecular geometries of meridional and facial Alq_3 were optimized at DFT using the B3LYP functional, where Becke's three-parameter hybrid exchange functional[23−25] is combined with the Lee−Yang−Parr correlation functional.[26] The 6-31G(d) split valence plus polarization basis set was used, which is most frequently used for the geometry optimizations of these Alq_3 isomers.[9,12,27−29] The nuclear magnetic shielding calculations for the DFT-optimized meridional and facial Alq_3 single molecules were carried out by the gauge including atomic orbitals (GIAO) method[30−32] using DFT at the B3LYP/6-31G(d) level. The reliability of the calculated absolute chemical shielding values was unclear, and all the chemical shifts in this paper were referenced by the experimental isotropic chemical shift of C8 carbon of γ-Alq_3, which gave a single resonance line and was clearly separated from the other resonance lines. All the isotropic chemical shifts of meridional and facial Alq_3 molecules relative to the C8 resonance line are in reasonable agreement with the experimental chemical shifts as shown below. All the calculations for geometry optimizations and NMR chemical shifts were performed with the Gaussian 98 program.[33]

Table 1. Summary of the Fluorescence Maxima and the Local Structures for Different Alq_3 Samples in this Study

	α-Alq_3	γ-Alq_3	δ-Alq_3	amorphous Alq_3
fluorescence maximum	510 nm (2.43 eV)	468 nm (2.65 eV)	466 nm (2.66 eV)	509 nm (2.44 eV)
isomeric state	meridional[5]	facial	facial[7−14]	meridional
order/disorder	disordered	ordered	ordered	disordered
intermolecular interaction	strong	weak	strong	strong

Results and Discussion

Blue-Shift Emissions in γ- and δ-Alq_3. Table 1 shows the maximum wavelengths of the fluorescence measurements. The α-Alq_3 and amorphous Alq_3 are found to show similar fluorescence with the maximum wavelength of 510 and 509 nm, respectively. In contrast, γ- and δ-Alq_3 show blue-shifted spectra with the maximum wavelength of 468 and 466 nm, respectively. Figure 2 shows the corresponding photographs under room light (left column) and under UV irradiation with an excitation wavelength of 365 nm (right column). This figure clearly shows the difference; a blue-shifted emission is observed for γ- and δ-Alq_3.

Solution ^{13}C NMR Spectrum. Figure 3a shows the experimental ^{13}C NMR spectrum of Alq_3 in $CDCl_3$ solution. The expanded spectrum is shown in Figure 3b. All the carbon species, assigned as C2 to C10, show three well-resolved resonance lines, except for the C9 carbon. For C9 carbons, only two resonance lines are observed. However, the integrated intensities are nearly 1:2, indicating that two of the three signals happen to overlap. Therefore, Alq_3 is found to be in the meridional form in $CDCl_3$ solution as is already reported by solution ^{1}H NMR experiments.[22] The three-line splittings are observed in solution ^{1}H and ^{13}C NMR spectra of all the Alq_3 samples including γ- and δ-Alq_3, indicating that Alq_3 becomes meridional on dissolving it into $CDCl_3$. Therefore, the isomeric state should be investigated directly in the solid state. Among all the carbon species, C8, C2, and C3 resonance lines are well separated from the other resonance lines. The C2 carbon shows the largest splitting with 2.56 ppm (255 Hz), and in the

(21) Baker, B. C.; Sawyer, D. T. *Anal. Chem.* **1968**, *40*, 1945−1951.
(22) Utz, M.; Chen, C.; Morton, M.; Papadimitrakopoulos, F. *J. Am. Chem. Soc.* **2003**, *125*, 1371−1375.
(23) Becke, A. D. *Phys. Rev. A* **1988**, *38*, 3098−3100.
(24) Becke, A. D. *J. Chem. Phys.* **1993**, *98*, 1372−1377.
(25) Becke, A. D. *J. Chem. Phys.* **1993**, *98*, 5648−5652.
(26) Lee, C. T.; Yang, W. T.; Parr, R. G. *Phys. Rev. B* **1988**, *37*, 785−789.
(27) Bulovic, V.; Gu, G.; Burrows, P. E.; Forrest, S. R.; Thompson, M. E. *Nature* **1996**, *380*, 29.
(28) Sugimoto, M.; Sakaki, S.; Sakanoue, K.; Newton, M. D. *J. Appl. Phys.* **2001**, *90*, 6092−6097.
(29) Amati, M.; Lelj, F. *Chem. Phys. Lett.* **2002**, *363*, 451−457.
(30) Ditchfield, R. *Mol. Phys.* **1974**, *27*, 789−807.
(31) Wolinski, K.; Hinton, J. F.; Pulay, P. *J. Am. Chem. Soc.* **1990**, *112*, 8251−8260.
(32) Rauhut, G.; Puyear, S.; Wolinski, K.; Pulay, P. *J. Phys. Chem.* **1996**, *100*, 6310−6316.
(33) Frisch, M. J.; Trucks, G. W.; Schlegel, H. B.; Scuseria, G. E.; Robb, M. A.; Cheeseman, J. R.; Zakrzewski, V. G.; Montgomery, J. A., Jr.; Stratmann, R. E.; Burant, J. C.; Dapprich, S.; Millam, J. M.; Daniels, A. D.; Kudin, K. N.; Strain, M. C.; Farkas, O.; Tomasi, J.; Barone, V.; Cossi, M.; Cammi, R.; Mennucci, B.; Pomelli, C.; Adamo, C.; Clifford, S.; Ochterski, J.; Petersson, G. A.; Ayala, P. Y.; Cui, Q.; Morokuma, K.; Malick, D. K.; Rabuck, A. D.; Raghavachari, K.; Foresman, J. B.; Cioslowski, J.; Ortiz, J. V.; Stefanov, B. B.; Liu, G.; Liashenko, A.; Piskorz, P.; Komaromi, I.; Gomperts, R.; Martin, R. L.; Fox, D. J.; Keith, T.; Al-Laham, M. A.; Peng, C. Y.; Nanayakkara, A.; Gonzalez, C.; Challacombe, M.; Gill, P. M. W.; Johnson, B. G.; Chen, W.; Wong, M. W.; Andres, J. L.; Head-Gordon, M.; Replogle, E. S.; Pople, J. A. *Gaussian 98*, revision A.11; Gaussian, Inc.: Pittsburgh, PA, 2001.

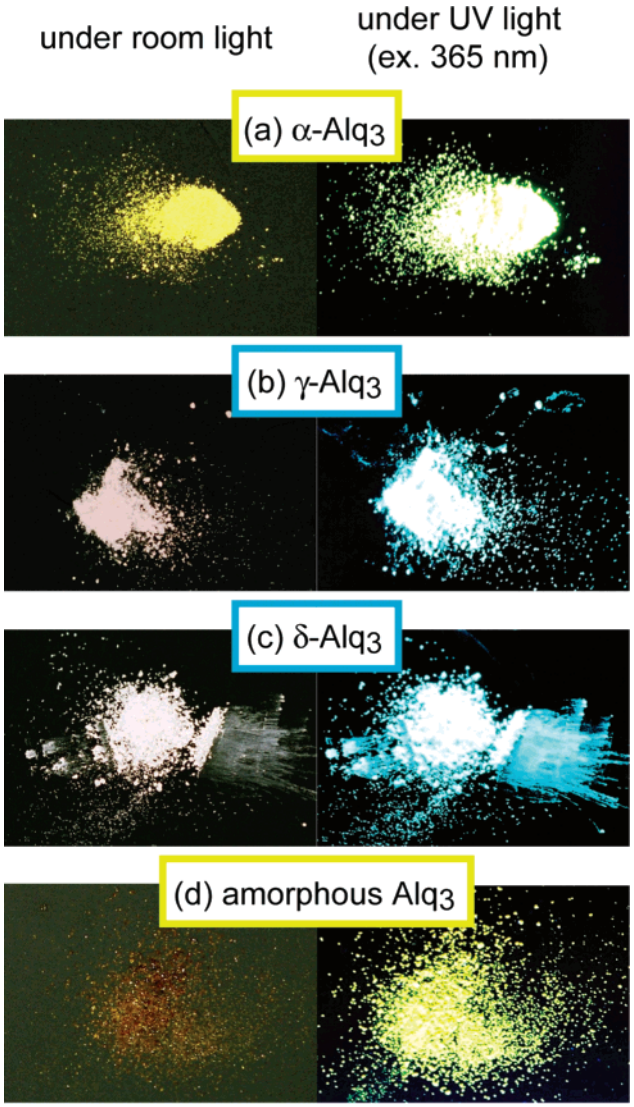

Figure 2. Photographs of (a) α-, (b) γ-, (c) δ-, and (d) amorphous Alq_3 under room light (left column) and UV-irradiation at an excitation wavelength of 365 nm (right column). The γ- and δ-Alq_3, which are whitish under room light, show clear blue-shifted luminescence under UV-irradiation.

following, therefore, we mainly use C2 signals as an indicator for distinction of the local structures.

CP/MAS ^{13}C NMR Spectra. Figure 4 shows the experimental CP/MAS ^{13}C NMR spectra of Alq_3 in different states along with the solution spectrum for reference at the top. The DFT-calculated ^{13}C isotropic chemical shifts of Alq_3 in the two isomeric forms are also shown. The DFT-calculated resonance lines of the meridional Alq_3 in Figure 4f split into three for the respective carbon species such as the solution ^{13}C NMR spectrum (see Figure S5 in the Supporting Information for details), whereas those of the facial Alq_3 in Figure 4g show single resonance lines.

For α-Alq_3 in Figure 4b, the resonance lines of the respective carbons are broadly distributed compared with those of the solution spectrum and DFT-calculations. The distributions of the resonance lines indicate the existence of structural disorders. Note that the α-Alq_3 sample shows sharp reflections in WAXD diffraction patterns, and therefore, the disorder is only local. Both the intramolecular origin and intermolecular origin are

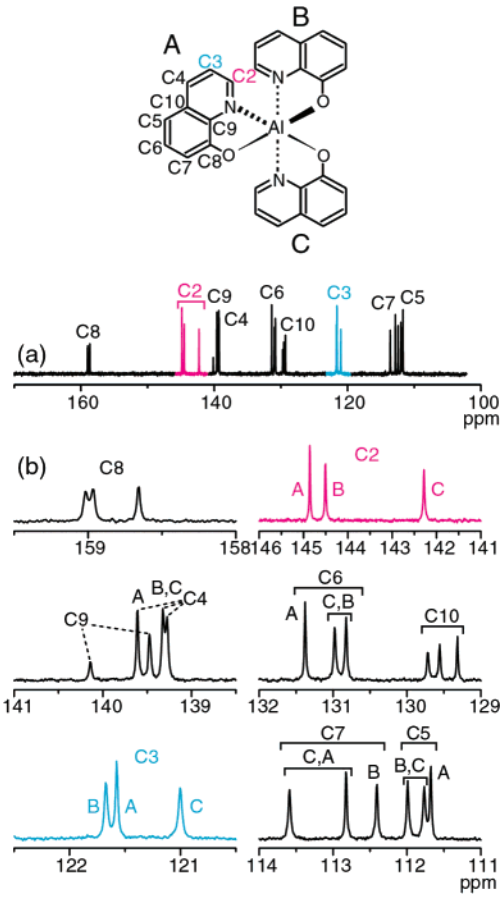

Figure 3. (a) Experimental solution ^{13}C NMR spectrum of Alq_3 dissolved in $CDCl_3$. The expanded spectrum is shown in (b).

considered.[7] The existence of the distribution of intramolecular structure is suggested by the DFT calculations.[2] In this calculation, the bond angles around the Al atom are shown to be distributed. The distribution of intermolecular packing is suggested by Raman spectra,[8] transmission electron microscopy (TEM),[15] and solid-state ^{27}Al NMR.[7] Similar spectral patterns of α-Alq_3 and amorphous Alq_3 in Figure 4 also suggest the existence of local disorder in α-Alq_3 as shown below.

The spectra of γ- and δ-Alq_3 in Figure 4c and d are drastically different from that of α-Alq_3. The γ- and δ-Alq_3 exhibit significantly sharp lines, indicating that the local structural disorder does not exist in these samples. The splitting of the resonance lines is expected by the intermolecular packing, such as ligand $\pi-\pi$ stacking. However, each carbon species of γ-Alq_3 shows a significantly sharp single resonance line. The C2 carbon exhibits a single Lorentian line shape with a line width (fwhm) of 51.0 Hz, and splittings due to both the intermolecular packing and the intramolecular interaction are not observed. This result clearly indicates that the γ-Alq_3 is in the facial isomeric state where the three ligands attached to an Alq_3 molecule are equivalent. This identification is confirmed by the resonance lines of all the other carbon species in Figure 4c, which also show sharp and single resonance lines with line widths of 24.8–44.2 Hz.

For δ-Alq_3, the resonance lines are found to split due to the intermolecular packing. Especially for the C2 carbon, three clear equally spaced resonance lines are observed. The splitting does not originate from the intramolecular interaction of the meridional isomer, because the δ-Alq_3 is already found to be facial.[7–14]

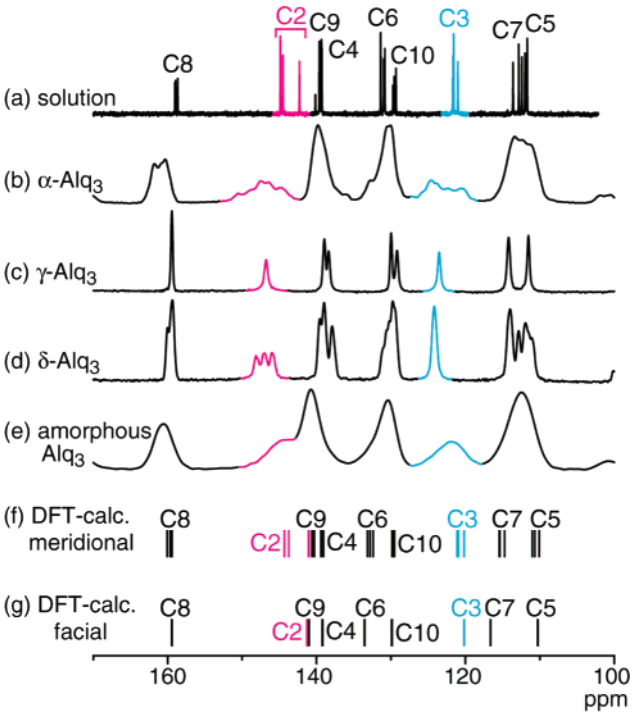

Figure 4. Experimental CP/MAS ^{13}C NMR spectra of (b) α-, (c) γ-, (d) δ-, and (e) amorphous Alq_3. In (f) and (g), DFT-calculated isotropic resonance lines are shown as vertical bars for meridional and facial Alq_3, respectively. The solution ^{13}C NMR spectrum of Alq_3 is also shown in (a) for reference.

The intramolecular interaction of the meridional isomer causes the unequally spaced resonance line splitting, and the most upfield C2C resonance line is substantially separated from the other two, C2A and C2B resonance lines, as is found from the solution NMR spectrum and the DFT-calculated isotropic chemical shifts (see Figure 3b and Figure S5b). This unequally spaced resonance line splitting is easily understood by the difference in the environment of the three C2 carbons. The DFT calculation reveals that the C2C carbon is located near the nitrogen in the adjacent quinolinol ring, whereas the C2A and C2B carbons are located near the oxygens. That is, the local environments of the C2A and C2B carbons are similar, whereas that of the C2C carbon is quite different. This trend is more clearly observed in the solution ^1H NMR spectrum in Figure S1, where H2C resonance lines are significantly separated from H2A and H2B resonance lines (see Figure S4 for the relation of ^1H and ^{13}C resonance lines). Therefore, we can conclude that the equally spaced resonance line splitting in Figure 4d originates from the intermolecular interaction. This conclusion agrees with the ^{27}Al NMR and infrared (IR) experiments.[7,34] In contrast to the dipolar decoupled MAS ^{27}Al NMR spectrum of γ-Alq_3, which can be explained by a single Alq_3 molecule in the facial form, the intermolecular interaction should be considered to explain the dipolar decoupled MAS ^{27}Al NMR spectrum of δ-Alq_3.[7] In the IR experiment, a similar peak splitting is observed for δ-Alq_3, which is also considered to originate from the intermolecular interaction.[34]

Figure 4e shows the CP/MAS ^{13}C NMR spectrum of amorphous Alq_3. The spectrum with broad resonance lines is similar to that of α-Alq_3 and is distinctly different from the sharp spectral patterns of γ- and δ-Alq_3. On the basis of the X-ray diffraction measurements, α-Alq_3 shows sharp diffraction patterns, whereas amorphous Alq_3 shows only an amorphous halo, indicating that the long-range order is significantly different between the two. However, the present solid-state NMR measurements clearly indicate that the local structures of α-Alq_3 and amorphous Alq_3 are very similar. The isomeric state of α-Alq_3 is already determined to be meridional.[5] Therefore, Alq_3 in the amorphous state is found to be mainly composed of the meridional state. Similar spectral patterns between α-Alq_3 and amorphous Alq_3 in turn confirm the existence of local structural disorder even in α-Alq_3. The isomeric state and local structural disorder concluded in this study agree with the previously reported ^{27}Al NMR experiments. In more detail, upfield-shifts of C2 resonance lines and different resonance line patterns for the C3 carbon in amorphous Alq_3 are found, although all the other resonance lines are similar for α- and amorphous Alq_3. The difference suggests some structural modifications between these Alq_3 samples, which are not observed in ^{27}Al NMR measurements. To completely understand the differences, we are now planning advanced solid-state NMR experiments[35−38] using isotopically ^{15}N or ^{13}C-labeled Alq_3 samples.

As shown above, the CP/MAS ^{13}C NMR spectra of α-, δ-, and amorphous Alq_3 are found to be affected by the intermolecular interaction. In contrast, no intermolecular effect is found for γ-Alq_3. Two possibilities are considered as the reason. One is that the intermolecular interaction in γ-Alq_3 is too weak to affect the solid-state NMR spectrum, and the other is that the resonance lines do not split due to the symmetry of the crystal packing. The better solvent solubility of γ-Alq_3 compared with α- and δ-Alq_3 was already found,[7] and this suggests a weaker intermolecular interaction for γ-Alq_3.

Our experimental results show that amorphous Alq_3 is composed predominantly of the meridional isomer. This is consistent with the results of solid-state ^{27}Al NMR[7,13] and matrix-isolated infrared measurement.[4] However, amorphous samples with different local structures are expected to be formed by different preparation schemes for amorphous samples, in particular, the condition of vacuum deposition, such as deposition rate, substrate temperature, etc. Different fluorescence maxima are reported for amorphous Alq_3 with different preparation conditions. Brinkmann et al.[5,15] show fluorescence maxima of 541 and 526 nm for sublimed amorphous films with substrate temperatures of 300 and 375 K, respectively. Cölle et al.[11,14] show fluorescence maxima of 537 and 519 nm for an amorphous sample quenched from the melt into liquid nitrogen and a sublimed amorphous film, respectively. Our amorphous sample quenched from the melt into ice−water shows a fluorescence maximum of 509 nm. These differences are expected to originate from the local structure modification in amorphous Alq_3 samples. Therefore, solid-state NMR measurements of amorphous samples with different preparation conditions are necessary to clarify the amorphous structures with different light-emitting/electron-transport properties. The clarification of the detailed amorphous structures will provide a guideline for fabricating Alq_3 thin films with better properties.

(34) Cölle, M.; Forero-Lenger, S.; Gmeiner, J.; Brütting, W. *Phys. Chem. Chem. Phys.* **2003**, *5*, 2958−2963.
(35) Schmidt-Rohr, K. *Macromolecules* **1996**, *29*, 3975−3981.
(36) Schmidt-Rohr, K.; Hu, W.; Zumbulyadis, N. *Science* **1998**, *280*, 714−717.
(37) Kaji, H.; Schmidt-Rohr, K. *Macromolecules* **2001**, *34*, 7368−7381.
(38) Kaji, H.; Schmidt-Rohr, K. *Macromolecules* **2002**, *35*, 7993−8004.

The maximum fluorescence wavelengths and the local structures of Alq_3 samples in this study are summarized in Table 1. A close relation between the isomeric states and the light-emitting properties is concluded from the CP/MAS ^{13}C NMR results. The facial isomers show 41−44 nm (0.21−0.23 eV) blue-shifted fluorescence compared with the meridional isomers. This indicates that the fluorescence wavelength of Alq_3 is mainly determined by the intramolecular isomeric states. The intermolecular interactions are significantly different between the two facial polymorphs, γ- and δ-Alq_3, as found from the CP/MAS ^{13}C NMR spectra. However, the photoluminescence (PL) spectra of these samples are similar, indicating that the effect of intermolecular interaction is negligible for the facial isomers. For the meridional isomer, Brinkmann et al. consider that the fluorescence maximum is correlated with $\pi-\pi$ interligand interaction[5] or sample densities.[15] They show a relation between the fluorescence maxima and the densities of Alq_3 and tris(8-hydroxyquinoline) gallium(III).[15] However, the change in the fluorescence maxima due to the densities is smaller compared with that by the isomeric effect. In our study, the differences in the C2 chemical shifts and the C3 spectral patterns in Figures 4b and e reflect some difference in the local intermolecular packing in α- and amorphous Alq_3 samples. However, the difference does not significantly influence the PL character. Therefore, we can conclude that the fluorescence wavelengths are mainly determined by the isomeric states of Alq_3 molecules and are modulated by the intermolecular interaction. We should note that the 0.21−0.23 eV difference between meridional and facial Alq_3 in this study is close to the difference in the DFT-calculated HOMO−LUMO gaps, 0.3 eV, between meridional and facial Alq_3 molecules.[2] The DFT calculations were carried out for single molecules; thus the difference is purely from the intramolecular origin.

Conclusions

The local structures of crystalline Alq_3 in the different polymorphs and amorphous Alq_3 have been analyzed by CP/MAS ^{13}C NMR spectroscopy. All the resonance lines in the CP/MAS ^{13}C NMR spectrum of α-Alq_3 are widely distributed, indicating the local disorder in the meridional α-Alq_3 structure. In contrast, γ-Alq_3 shows sharp single resonance lines for the respective carbons, and we conclude that the local structure of γ-Alq_3 is well-ordered and that γ-Alq_3 is attributed to the facial isomer in which the three ligands are magnetically equivalent. No effects of intermolecular interactions are found. This finding can explain the good solvent solubility of γ-Alq_3, compared with the other crystalline forms. The resonance lines of δ-Alq_3, which is already known to be facial, are also sharp but are split due to the intermolecular interaction. The CP/MAS ^{13}C NMR spectrum of amorphous Alq_3 is quite similar to that of α-Alq_3, indicating similar local structures. The meridional isomer is suggested to be dominant in the amorphous Alq_3, although more detailed experiments are necessary for the quantitative determination of the existence of the facial isomers. It is also found that the fluorescence wavelengths are primarily determined by the isomeric states and are modulated by the intermolecular packing.

Acknowledgment. We thank Professor M. Takano and Professor M. Azuma for the WAXD measurements. H.K. also thanks Prof. H. Murata for his helpful advice. The computation time was provided by the Supercomputer Laboratory, Institute for Chemical Research, Kyoto University.

Supporting Information Available: Solution and DFT-calculated NMR spectra for the signal assignments and a complete author list for ref 33 (PDF). This material is available free of charge via the Internet at http://pubs.acs.org.

JA0565774